

# Time-of-Flight Measurements with MCP-PMT

K. Inami

Department of Physics, Nagoya University, Nagoya 464-8602, Japan

The performance of micro-channel-plate photo-multiplier-tubes (MCP-PMT's) was measured. We here report on two interesting results among many: One is on a specific time-of-flight (TOF) counter that achieved a time resolution of  $\sigma = 6$  ps; the other is on an effect of employing an ion-feedback prevention layer to lengthen the MCP-PMT's lifetime.

## 1. Introduction

Aiming at a new particle ( $K/\pi$ ) identification device for a super KEKB-factory experiment, we have been developing a high identification power and quite compact Cherenkov ring imaging device, named time-of-propagation (TOP) counter [1]. It requires a photo-device to provide a timing resolution of  $\sigma_{TTS} \simeq 50$  ps and to be single-photon sensitive and position detectable. Further, it is operational under a 1.5 T magnetic field strength, and has a high detection efficiency. Some of MCP-PMT's, we developed under a collaboration with Hamamatsu Photonics Co. (HPK) satisfy those requirements. (Concerning our MCP-PMT's, see [2, 3].)

With the use of such an MCP-PMT, a small TOF counter was constructed and beam-tested. It obtained a superb time resolution, as reported in section 2.

While an MCP-PMT generally provides superb performances as a photo-device compared to an ordinary vacuum PMT, or other kinds of devices, its lifetime under a high-rate circumstance has not been well studied and controlled; rather, it is considered to be insecure. We tested the lifetimes for several types of MCP-PMT's by irradiating with light pulses over several (more than 10) years of expected super KEKB experimental circumstance. In the section 3, we report on the importance of setting an ion-feedback prevention layer for sufficiently lengthening the lifetime, compared to those of MCP-PMT's without the layer.

## 2. A Fast TOF counter

For an ordinary TOF scintillation counter, the timing resolution ( $\sigma_{TOF}$ ) is limited mostly by a long scintillating decay constant, for instance, a few ns at a plastic scintillator, as well as dispersive light path-lengths, in spite of its large number of scintillation light quanta. On the other hand, Cherenkov radiation provides some advantages: Light is emitted within a practically zero time duration when a charged particle passes through a radiator; the light has an angle of  $\sim 45^\circ$  relative to a relativistic particle so that a specific geometrical configuration of a radiator, such as our counter discussed below, makes light passages

not influential in gaining precise timing information. To realize these profits, a fast photo-device, such as the MCP-PMT, is required.

### 2.1. TOF counter

A TOF counter is composed of a small-size of quartz ( $n = 1.47$ ) radiator and an MCP-PMT, as illustrated in Fig. 1. Quartz with a size of  $16 \text{ mm} \times 16 \text{ mm} \times 40 \text{ mm}^L$  was employed as a radiator, on one end of which a MCP-PMT was mounted and the others were aluminum coated by vacuum evaporation.

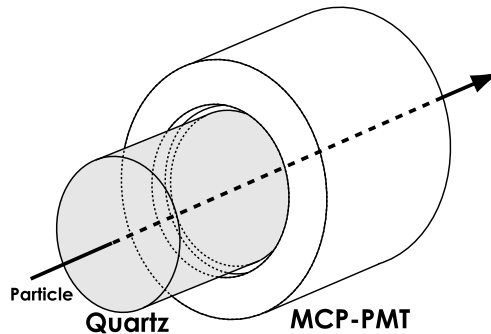


Figure 1: Schematic drawing of the TOF counter.

The time resolution would mostly involve the following three contributions:

$$\sigma_{TOF} = \sigma_\ell \oplus \sigma_{MCP} \oplus \sigma_{circuit}.$$

(See below for explanations on each term.)

The arrival time of Cherenkov light, produced along the passage of a particle, hits perpendicular to the quartz, at MCP-PMT spreads of over  $\sim 30 \times \ell$  (ps), where  $\ell$  is the length (cm) of the quartz; its root-mean-spread is  $\sigma_\ell \sim 30 \times \ell / (\sqrt{12} \sqrt{n_{p.e.}})$  (ps), where  $n_{p.e.}$  is a number of detected photo-electrons. Since  $n = 40\text{-}50$  p.e./ $\ell$  at the TOF counter,  $\sigma_\ell \sim 1.3\sqrt{\ell}$ .

The transit time spread (TTS) of our MCP-PMT is around  $\sigma_{TTS} = 30\text{-}50$  ps, so that TTS fluctuation contributes by  $\sigma_{MCP} \sim \sigma_{TTS} / \sqrt{n_{p.e.}} \sim (5 - 8) / \sqrt{\ell}$ .

The third contribution, the ambiguity ( $\sigma_{circuit}$ ) in the timing determination of readout circuits, predominates the achievable resolution in our case, as discussed in the next subsection.

Two types of MCP-PMT's were used as the photo-device. They were two-stage MCP-PMT with multi-alkali photocathode (quantum efficiency ( $QE$ )  $\sim 20\%$  at  $\lambda \sim 400$  nm). One was a Hamamatsu R3809U-50-25X (HPK10) with a channel diameter of  $10 \mu\text{m}$ , the other was a R3809U-50-11X (HPK6) with  $6 \mu\text{m}$ . Figs. 2 shows the ADC and TDC spectra for single photo-electrons. These MCP-PMTs exhibit a sufficiently large gain of  $\mathcal{O}(10^6)$  under the normal operating condition to obtain time resolutions of  $\sigma_{\text{TTS}} = 46$  ps and  $30.4$  ps, respectively.

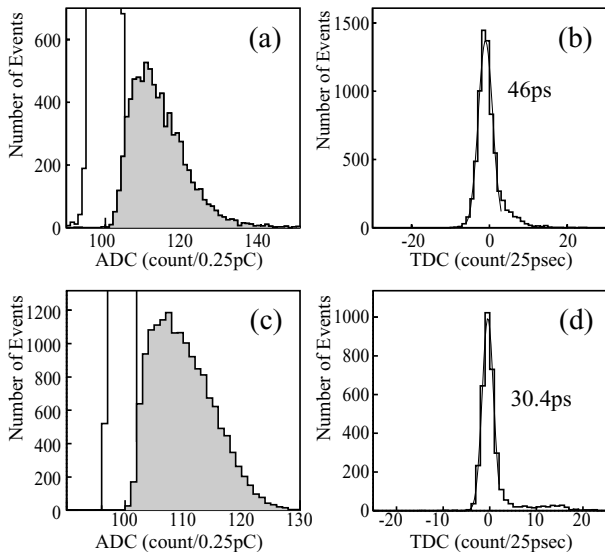


Figure 2: ADC and TDC (time-walk corrected) spectra: (a) and (b) are of Hamamatsu R3809U-50-25X, and (c) and (d) are of R3809U-50-11X, respectively, for single photo-electrons.

## 2.2. With NIM & CAMAC modules

A beam-test was performed using a  $3 \text{ GeV}/c \pi^-$  beam at the KEK-PS  $\pi 2$  line. Fig. 3 illustrates the setup for the beam test. Two TOF counters with HPK10 were located between two small scintillation counters for triggering and beam defining. The size of scintillator was  $5 \text{ mm} \times 5 \text{ mm} \times 10 \text{ mm}^L$ . The distance between two TOF counters was  $30 \text{ cm}$ .

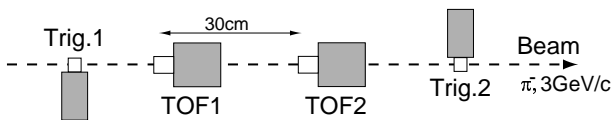


Figure 3: Setup of beam tests.

The readout system was composed of discriminators (Phillips Scientific model 708) and ADC ( $0.25 \text{ pC}/\text{count}$ ) and TDC ( $25 \text{ ps}/\text{count}$ ) CAMAC modules.

Its resolution was measured to be  $\sigma_{\text{circuit}} = 7\text{-}9$  ps using pulser signals.

Figs. 4 show the observed time-difference distributions between two TOF counters after a time-walk correction. The spectrum (a) was obtained with an  $\ell = 40$  mm quartz radiator. The number of detected photo-electrons was  $n_{p.e.} \sim 250$ , which agreed with the expected simulation result of  $\sim 240$ . The time resolution was  $\sigma_{\text{TOF}} = 10.6$  ps.

Without the quartz radiator,  $n_{p.e.}$  was measured to be  $\sim 50$ . These photons might be Cherenkov light from the  $4 \text{ mm}$ -thick PMT quartz window, while its amount was 2-times larger than the expected.  $\sigma_{\text{TOF}} = 13.6$  ps was obtained, as shown in Fig. 4(b).

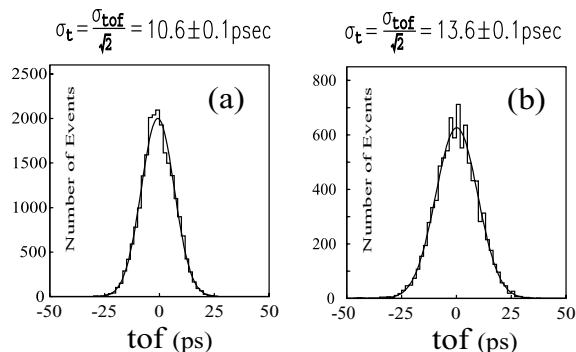


Figure 4: TOF resolutions of the first beam test with a  $40 \text{ mm}$ -thick quartz radiator (a) and without a radiator (b).

During the beam test,  $\sigma_{\text{circuit}}$  was measured as  $8.8$  ps, using signals from the MCP-PMT instead of pulser signals. Therefore, an intrinsic resolution of this TOF counter would be  $6$  ps: By having a more stable readout circuit, for instance,  $\sigma_{\text{circuit}} = 5$  ps, we can obtain  $\sigma_{\text{TOF}} = 7\text{-}8$  ps.

## 2.3. With a fast module

As a specific readout electronics module, we employed a time-correlated single-photon counting module (SPC-134), Becker & Hickl GmbH's, that exhibited a channel resolution of  $813 \text{ fs}$ , a time resolution of  $4 \text{ ps}$  in rms and repetition rates of up to  $200 \text{ MHz}$ . The system was composed of 4 modules, each of them comprising a constant fraction discriminator (CFD), a time-to-amplitude converter (TAC), an ADC and a multichannel analyzer (MCA). By using this system,  $\sigma_{\text{circuit}} \simeq 4$  ps, we could then examine the timing property of the TOF counter, itself.

The output signals of the counters were directly fed to SPC modules, as illustrated in Fig. 5(a). The coincidence between two trigger counters was prepared to give a stop timing signal for the SPC's. We took the difference between the TDC outputs of the two TOF counters in the analysis, so that the timing fluctuation

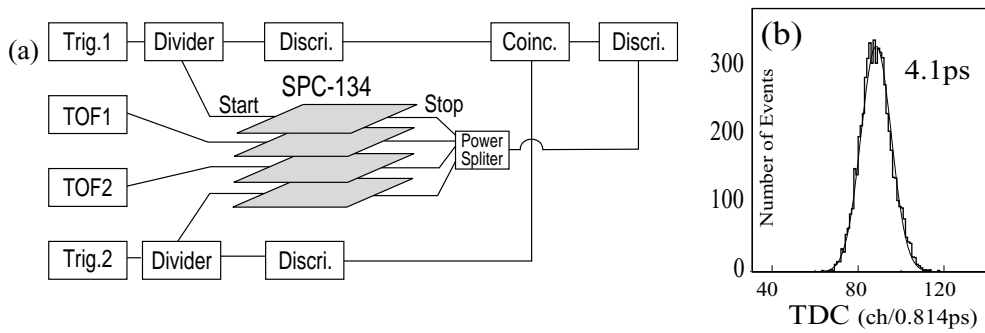


Figure 5: (a) Configuration of readout electronics, and (b) timing resolution of this system, measured with pulser signals.

of the stop signal was ineffective, as in the previous one. Fig. 5(b) shows the thus-obtained TOF spectrum for pulser signals:  $\sigma_{\text{circuit}} = 4.1$  ps.

Two TOF counters were prepared in the same way as the previous ones, but HPK10 ( $\sigma_{\text{TTS}} = 46$  ps and an  $\ell = 4$  mm window) was replaced by HPK6 ( $\sigma_{\text{TTS}} = 30$  ps and an  $\ell = 3$  mm window). Also, a cylindrical quartz of 10 mm $\phi$  with different  $\ell$  was attached in front of the HPK6. The setup for the beam-test was the same as the previous one, as shown in Fig. 3.

Figs. 6 show the TOF spectrum for the counters (a) with and (b) without an  $\ell = 10$  mm quartz for a 3 GeV/c  $\pi$  beam. The best resolution of  $\sigma_{\text{TOF}} = 6.2$  ps was attained with an  $\ell = 10$  mm quartz; the number of detected photo-electrons was  $n_{p.e.} \sim 180$ . However, without the quartz,  $\sigma_{\text{TOF}} = 7.7$  ps and  $n_{p.e.} \sim 80$ .

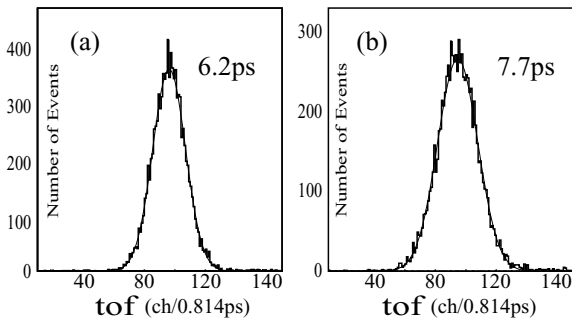


Figure 6: TOF resolutions of the second beam test with  $\ell = 10$  mm d quartz radiator (a) and without a radiator (b).

By changing  $\ell$ ,  $\sigma_{\text{TOF}}$  and  $n_{p.e.}$  were measured, as plotted in Figs. 7(a) and (b), respectively, where the closed circles and squares are data, and the open circles are results of a Monte-Carlo simulation. The GEANT program was employed to simulated the interactions of pions with the quartz, in which effects of emitted  $\delta$ -rays were included. Also, for the thus-obtained Cherenkov photons, their propagation of the quartz and the response of the MCP-PMT were simulated by our own developed program.

$n_{p.e.}$  was evaluated by comparing the amplitude of

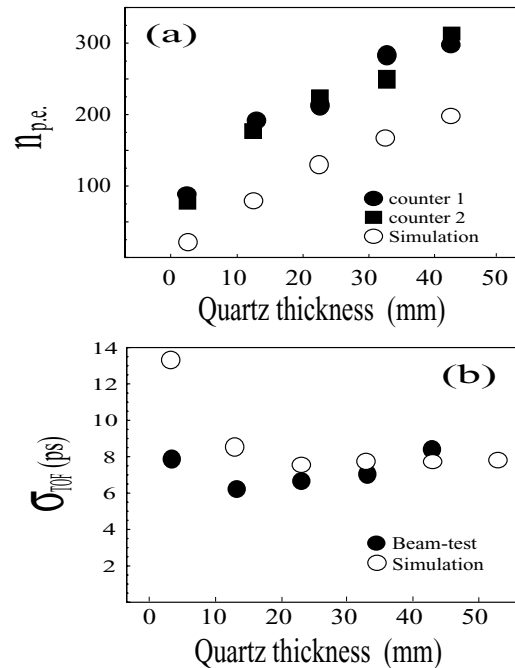


Figure 7:  $n_{p.e.}$  and  $\sigma_{\text{TOF}}$  dependence on the quartz thickness. The closed and open circles are the observed data and by a Monte-Carlo simulation, respectively.

the beam signals to that of the single photons from the pulser.  $n_{p.e.} \sim 20$  was expected for the  $\ell = 3$  mm-thick window, while we measured  $n_{p.e.} \sim 70$ -80. As is seen in Fig.7(a), the observed  $n_{p.e.}$  is largely different from the expected one: Both have a similar rate of  $\sim 50$  p.e./10 mm, but the former has an offset of  $\sim 70$ -80. This behavior is consistent with our previous measurement.

The best resolution of  $\sigma_{\text{TOF}} = 6.2$  ps was attained with  $\ell = 13$  mm in total; also, at  $\ell > 13$  mm  $\sigma_{\text{TOF}}$  deteriorated with  $\ell$ , even though  $n_{p.e.}$  increased.

From these facts, we infer that extra photons might be emitted at an approximately close distance from the MCP-PMT face, and predominated the timing

resolution,  $\sigma_{\text{TOF}}$ .

### 3. Lifetime of MCP-PMT's

#### 3.1. Setup and ion-feedback prevention layer

Seven MCP-PMT's were tested. Their characteristics are listed in Table I. Two were manufactured by HPK, and the others were purchased from Budker Institute of Nuclear Physics (BINP). All MCP-PMT's had a multi-alkali photo-cathode, and were of the two-stage type; half of the MCP-PMT's were equipped with a prevention layer, and the other half were not. They were labeled by "w" and "wo", respectively.

The prevention layer was a thin aluminum film placed on the surface of the first MCP-layer at its photo-cathode side, so as to protect the photo-cathode from the feedback-ions produced in the multiplication process by collisions with residual gas or MCP plates. However, it inevitably introduced some transmission inefficiency for photo-electrons: It was typically about 40%, and accordingly caused a reduction of the photo-electron collection efficiency ( $CE$ ).

Under a supposition of the super KEKB collider with a luminosity of  $2 \times 10^{35}/\text{cm}^2/\text{s}$ , our specifically configured TOP counter would have a Cherenkov photon rate of  $680 \text{ kHz}/\text{cm}^2/\text{s}$  on an MCP-PMT. This corresponds to a total number of irradiated photons ( $n_\gamma$ ) over a one-year period of  $n_\gamma = 2.1 \times 10^{13} \text{ photons}/\text{cm}^2/\text{y}$  (we hereafter refer to this time period as one super-B year).

To simulate this circumstance, a blue LED ( $\lambda \simeq 400 \text{ nm}$ ) was pulsed by a rate of 1 - 5 kHz with a 10 ns-wide pulse: The irradiated photon rate was  $n_\gamma = 400\text{--}2,000/\text{pulse}$ . The light yields was calibrated by a  $QE$  well-known vacuum tube (HPK H3171-04). During continuous irradiation, we periodically measured the gain ( $G$ ),  $QE$ ,  $\sigma_{\text{TTS}}$  and dark-counts ( $n_{\text{dark}}$ ) of the MCP-PMT's for single photons generated by a picosecond light-pulsar ( $\lambda = 408 \text{ nm}$ ).

The variation of the MCP-PMT's performances was evaluated as a function of the integrated number of irradiated photons ( $n_\gamma$ ) or an integrated number of the output charges ( $Q$ ) from the MCP-PMT, over an area in units of  $\text{cm}^2$ . (Since  $Q$  reflects the MCP-PMT's performance, each MCP-PMT has a different  $Q$  value under a certain  $n_\gamma$ .)

#### 3.2. Gain, TTS and QE

Fig. 8 shows the relative gain variation,  $G$  vs  $n_\gamma$ . The initial gains can be found in Table I. Although HPK's and BINP-1w dropped their  $G$ 's fast at an early time period, all MCP-PMT's exhibited after this time quite stable behavior.

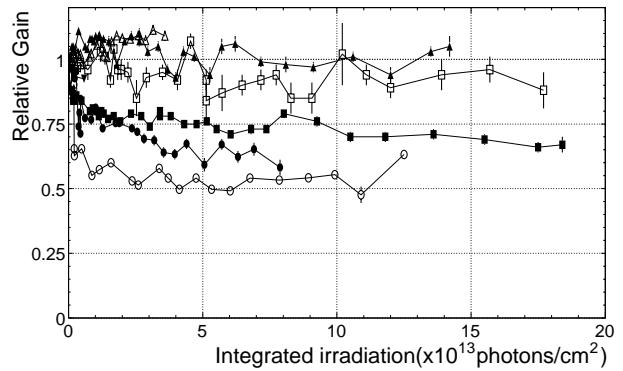


Figure 8: Relative gain variations under LED irradiation for all PMT's. The marks indicate HPK-w ( $\bullet$ ), HPK-wo ( $\circ$ ), BINP-1w ( $\blacksquare$ ), BINP-2w ( $\blacktriangle$ ), BINP-3w ( $\blacktriangledown$ ), BINP-4wo ( $\triangle$ ) and BINP-5wo ( $\square$ ).

Figs. 9 show the time-walk corrected TDC distributions before and after the lifetime test. No substantial difference on the distributions was found. The TTS variation was also measured during the testing period and found it to be stable.

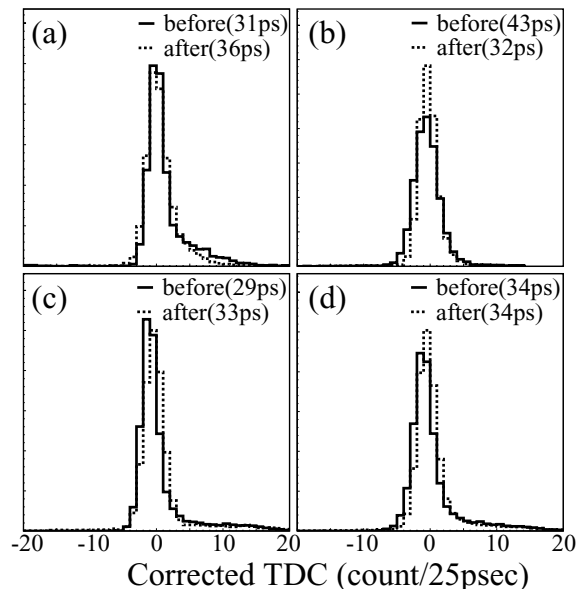


Figure 9: Corrected TDC distributions for (a) BINP-1w, (b) BINP-4wo, (c) HPK-w and (d) HPK-wo. The measured results before and after the lifetime test are indicated by the solid and dashed histograms, respectively.

Fig. 10 shows the relative  $QE$  variation at  $\lambda = 408 \text{ nm}$  as a function of  $n_\gamma$ .  $QE$  was measured as the ratio of the number of detected signals to the number of irradiated single-photons of laser pulser, whereas the  $CE$  was factored out.

Without the prevention layer,  $QE$  rapidly decreased to less than 50% within a tenth of a super-B year ( $Q < 100 \text{ mC}/\text{cm}^2$ ), and reached a few 10% after

Table I Characteristics of MCP-PMT's. All PMT's have a multi-alkali photo-cathode and two stages.

	HPK <sup>‡1</sup>		BINP <sup>‡1</sup>				
	-w	-wo	-1w	-2w	-3w	-4wo	-5wo
window	fused quartz		borosilicate glass				
diameter(mm) of effective area	11		18				
$QE$ (%) @ $\lambda = 400nm$	21	19	21	19	22	16	16
D <sup>‡2</sup> ( $\mu m$ )	6		6			8	
MCP aperture (%)	~ 60		~ 60			~ 45	
L <sup>‡2</sup> (mm)	0.24		0.30				
bias angle ( $^{\circ}$ )	13		5				
gap (mm) / voltage (V) between							
photo-cathode & 1st MCP-layer	2.0 / 970		0.7 / 1030			0.2 / 340	
1st & 2nd MCP-layers	0.51 / 1940		0.7 / 2450				
2nd MCP-layer & anode	1.0 / 480		0.3 / 130			1.2 / 110	
$HV$ supplied	3.4		3.6			2.9	
gain ( $\times 10^6$ )	1.5	1.9	4.0	2.9	3.2	4.1	2.9
$\sigma_{TTS}$ (ps)	29	34	31	44	54	44	36
dark counts (kHz)	1.5	0.38	40	300	64	14	20
$CE$ (%)	37	65	40	61	51	55	62

<sup>‡1</sup> PMT's with and without an ion-feedback prevention layer are labeled by "w" and "wo", respectively, in the individual tube numbers.

<sup>‡2</sup> D and L are the diameter and thickness of the MCP plate, respectively.

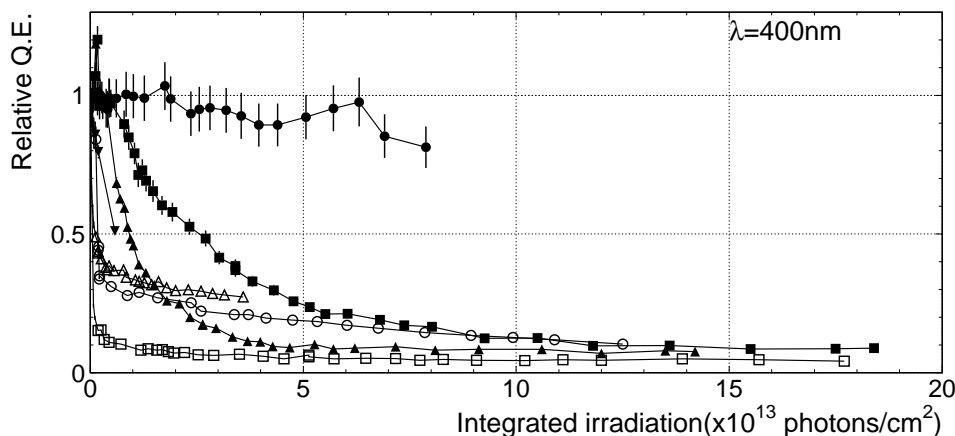


Figure 10: Relative QE variations under LED irradiation for all PMT's. The marks indicate HPK-w ( $\bullet$ ), HPK-wo ( $\circ$ ), BINP-1w ( $\blacksquare$ ), BINP-2w ( $\blacktriangle$ ), BINP-3w ( $\blacktriangledown$ ), BINP-4wo ( $\triangle$ ) and BINP-5wo ( $\square$ ).

one year. Even with the prevention layer equipped, BINP-2w and -3w exhibited a sharp drop, decreasing to  $<50\%$  at one half year ( $Q \simeq 500$  mC/cm<sup>2</sup>); BINP-1w showed a slightly slow drop, but reached  $\sim 60\%$  at one year ( $Q \simeq 600$  mC/cm<sup>2</sup>). Only HPK-w exhibited a gentle slope. It became around 90% after 4 super-B years ( $Q \simeq 1,000$  mC/cm<sup>2</sup>).

We measured the  $QE(\lambda)$  spectra after irradiation and compared it with the spectra before the test, as found in Figs. 11.  $QE$  at a short  $\lambda$  region exhibited a different behavior between HPK and BINP (see, Fig. 11(a)); the  $\lambda$  cutoff was  $\sim 160$  nm for fused quartz of HPK and  $\sim 300$  nm for Borosilicate of BINP. The  $QE(\lambda)$  ratio between after and before the irradi-

ation is shown in Fig. 11(b). It is common over all

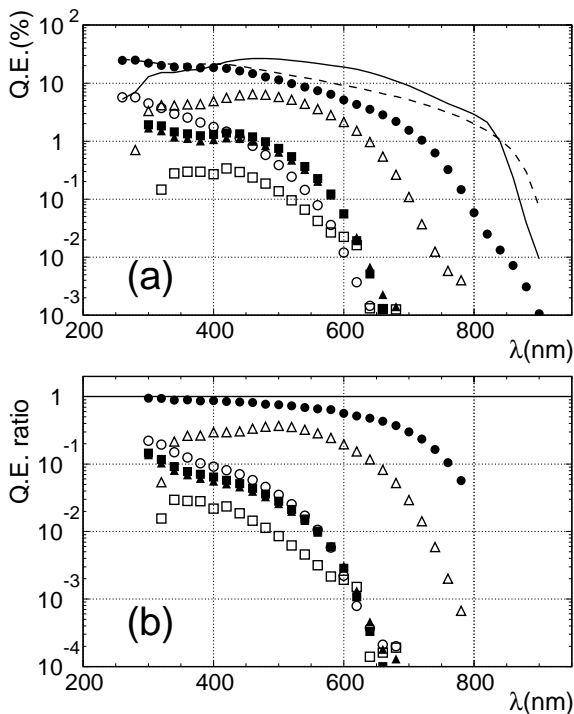


Figure 11: (a)  $QE(\lambda)$  after full irradiation, and (b)  $QE(\lambda)$  ratio between after and before irradiation. The solid line in (a) is the initial  $QE(\lambda)$  of HPK-w, and the dotted line is  $QE(\lambda)$  of another BINP-w PMT, not irradiated. The marks denote HPK-w ( $\bullet$ ), HPK-wo ( $\circ$ ), BINP-1w ( $\blacksquare$ ), BINP-2w ( $\blacktriangle$ ), BINP-3w ( $\blacktriangledown$ ), BINP-4wo ( $\triangle$ ) and BINP-5wo ( $\square$ ).

MCP-PMT's that the degradation of the  $QE$  ratio is much larger at longer  $\lambda$  than at shorter  $\lambda$ . HPK-w, which exhibits the smallest degradation among the seven MCP-PMT's, reduces the  $QE$  ratio to 30% at  $\lambda \sim 700$  nm, and 95% at  $\sim 300$  nm. It yields a 3-times difference in the  $QE$  ratio between the two  $\lambda$  regions. For other MCP-PMT's showing very sharp drops, 100-1,000 times differences in the  $QE$  ratio appear at  $\lambda = 300$ -700 nm.

### 3.3. Effect of ion-feedback prevention layer

Among the tested MCP-PMT's, only HPK-w satisfied our requirements and could function well under the super KEKB circumstance over several years, perhaps, around ten years. From a comparison between HPK-w and HPK-wo, it is stated that the ion-feedback prevention layer is essentially important to have a long lifetime. However, everyone doubts why BINP-w did not exhibit a long lifetime similar to HPK-w.

Two reasons can be noticed: Firstly, the fact that  $CE = 40$ -60% for BINP-w was much larger than 37%

for HPK-w, indicates that the higher transmission for photo-electrons would also hold for positive ions. The prevention layer might not effectively function for ions at BINP-w, compared to HPK-w. Secondly, the size of the bias-angle might play another important role. A smaller angle of  $5^\circ$  at BINP-w would not be sufficient to suppress the feedback, compared to  $13^\circ$  at HPK-w. (Please, refer Ref. [3] in more details. It shows and discusses the ion-feedback signal and its timing properties.)

## 4. Summary

MCP-PMT provides a high TTS of  $\sigma_{TTS} \simeq 30$  ps. With such an MCP-PMT, the specifically configured TOF counters with a small quartz, as a Cherenkov radiator, were prepared and we attained a time resolution of  $\sigma_{TOF} = 6.2$  ps with an ambiguity of the readout system of  $\sigma_{circuit} = 4.1$  ps.

The lifetimes of several MCP-PMT's were examined by measuring the variations of  $G$ , TTS and  $QE$  as a function of the integrated number of irradiated photons or the integrated output charges over certain time periods. Although some gain-drop occurred,  $\sigma_{TTS}$  was unaffected. The most critical effect appeared as  $QE$  degradation, that could not be recovered. The ion-feedback prevention layer effectively functioned in an MCP-PMT, HPK-w, protected the photo-cathode from positive ion-feedbacks.

For more details about the TOF counters and the lifetime measurements, see our papers [2-4].

## Acknowledgments

This work is supported by a Grant-in-Aid for Science Research on Priority Area, "Mass Origin and Supersymmetry Physics", from the Ministry of Education, Culture, Sports, Science and Technology of Japan.

## References

- [1] M. Akatsu *et al.*, Nucl. Instr. and Meth. **A 440** (2000) 124-135; T. Ohshima, Nucl. Instr. and Meth. **A 453** (2000) 331-335.
- [2] M. Akatsu *et al.*, Nucl. Instr. and Meth. **A 528** (2004) 763-775.
- [3] "Lifetime of MCP-PMT", N. Kishimoto *et al.*, to be published in Nucl. Instr. and Meth. **A**.
- [4] "A 5 ps TOF-counter with an MCP-PMT", K. Inami *et al.*, to be published in Nucl. Instr. and Meth. **A**.